Supporting Information

Hydrogenated Hematite Nanostructures for High-Efficiency Solar Water Oxidation

*Litao Zhou,[†] Xiaolin Lv,[†] Yuting Nie, Jiujun Deng, Hui Zhang, Xuhui Sun,*and Jun Zhong**

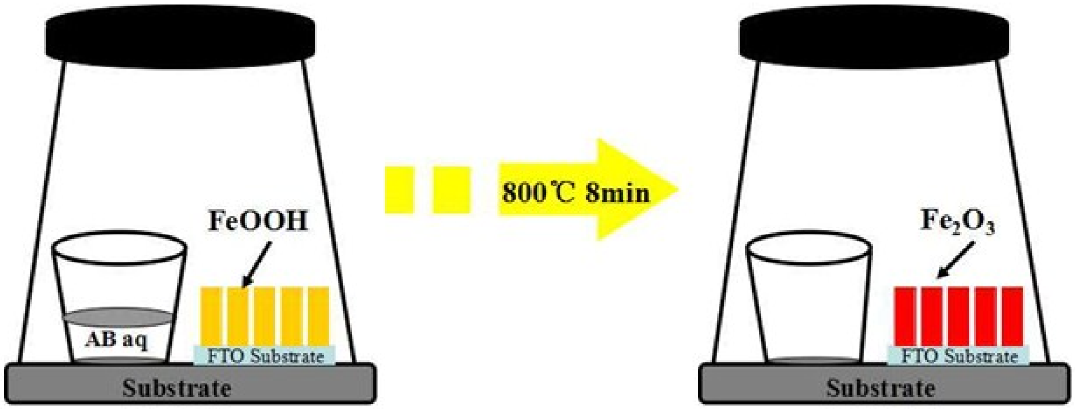

Figure S1: Experimental setup for the preparation of the AB-treated hematite.

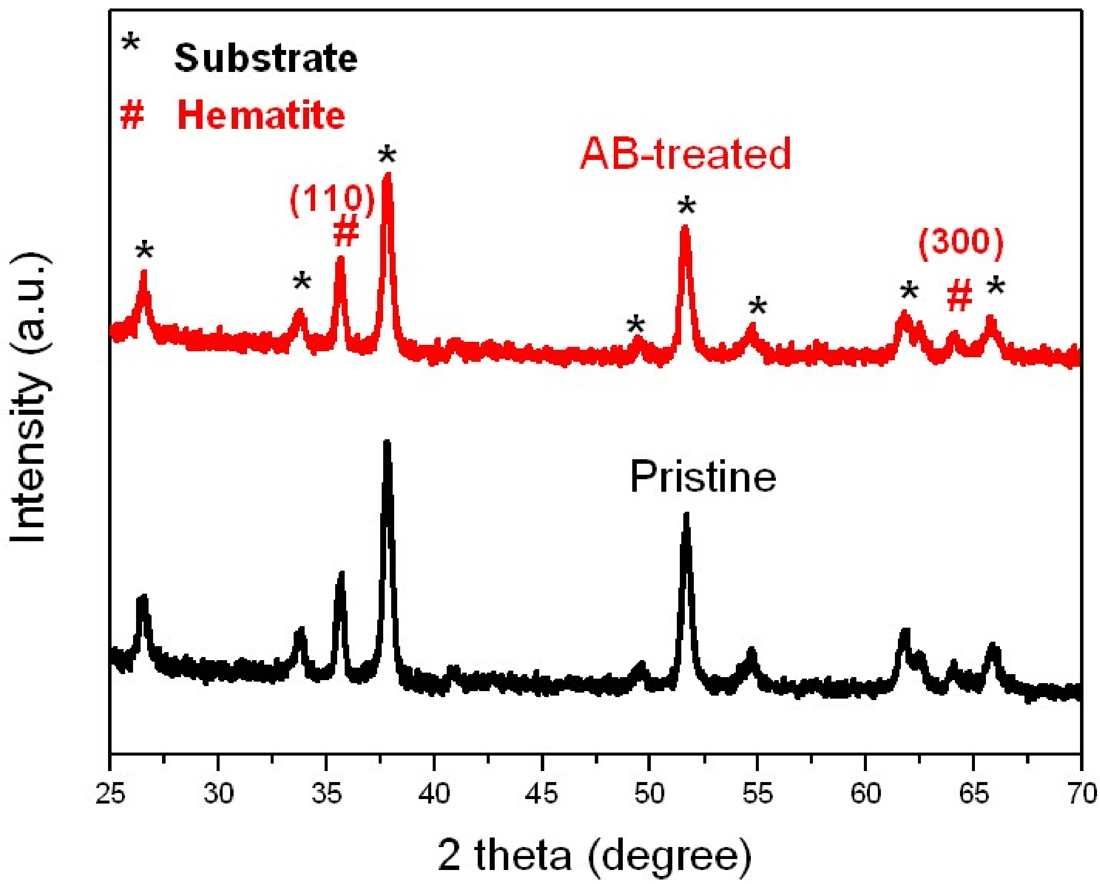

Figure S2: XRD spectra of the pristine and AB-treated hematite nanostructures.

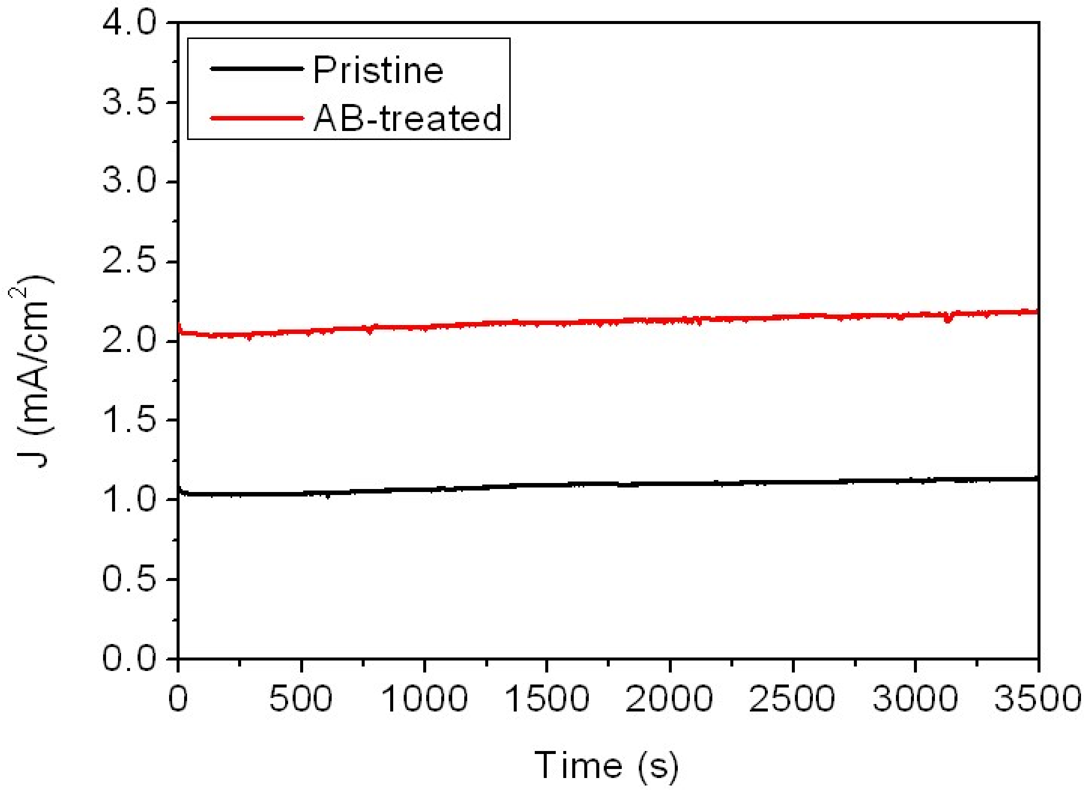

Figure S3: Photochemical stability curves of the pristine and AB-treated hematite photoanodes collected at 1.23 V vs. RHE.

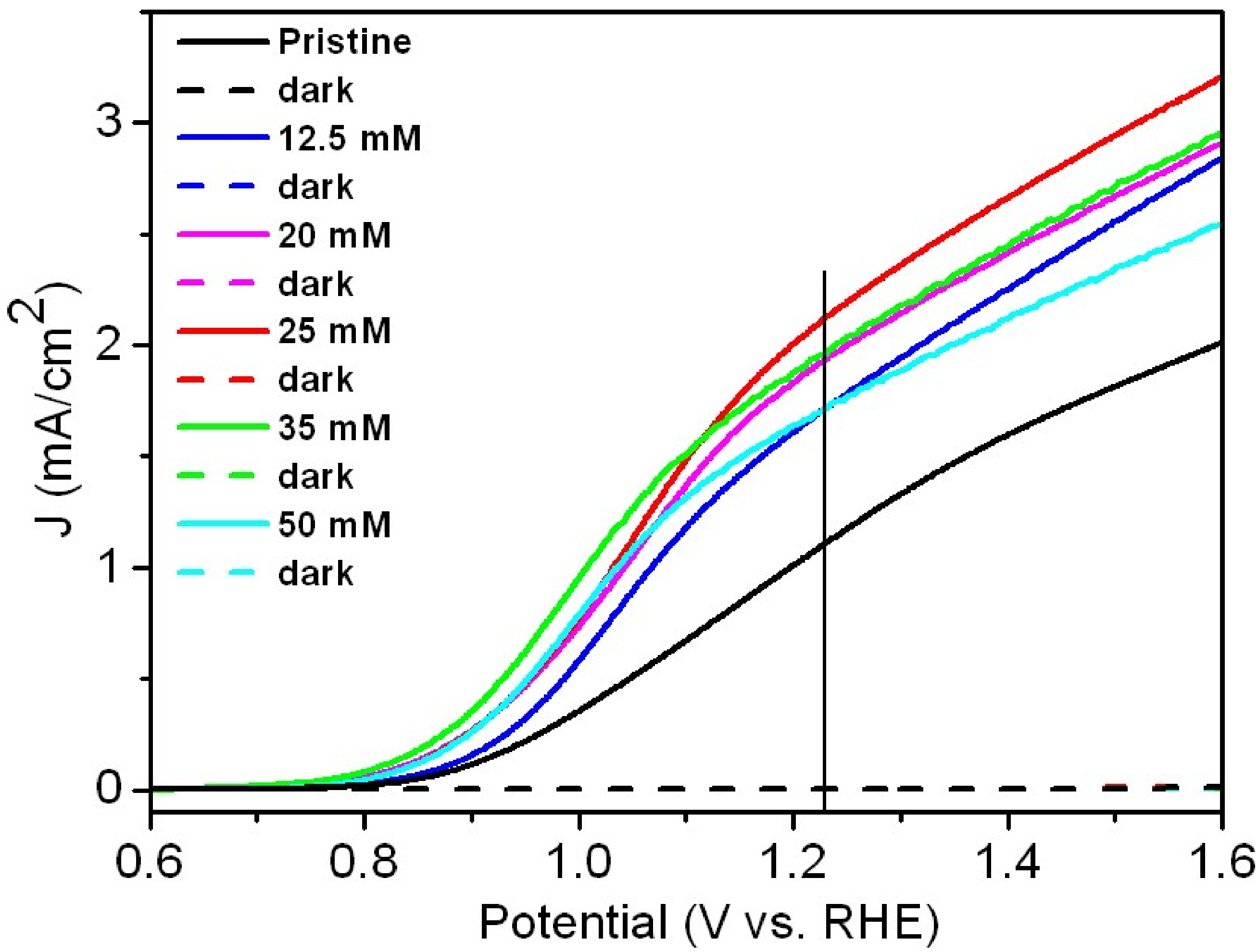

Figure S4: *J-V* scans of the AB-treated hematite photoanodes at various AB concentrations.

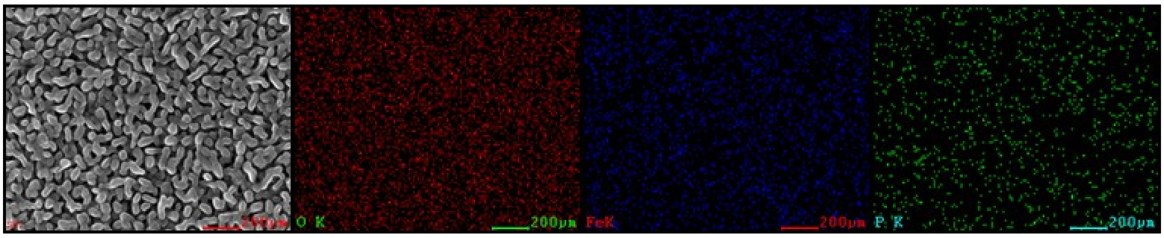

Figure S5: SEM image and the corresponding elemental mappings of the P-doped/AB-treated hematite photoanode. P mapping clearly confirms the P-doping in hematite.

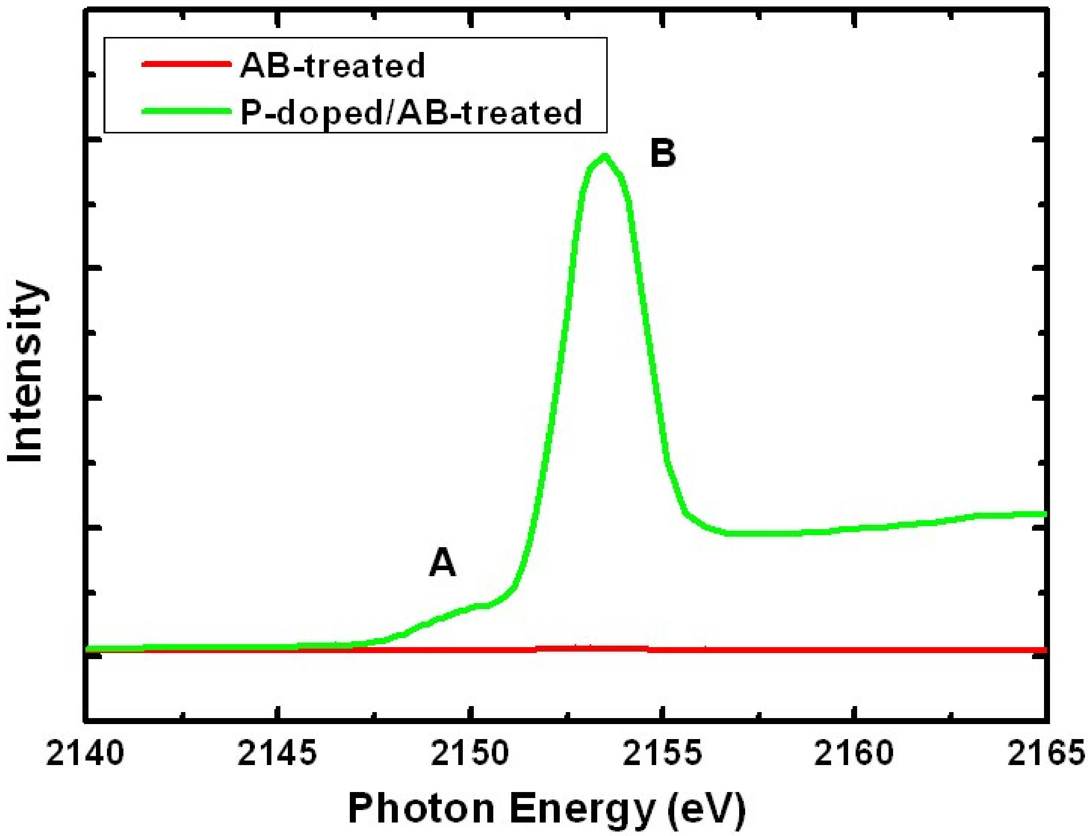

Figure S6: P *K*-edge XAS spectra of the AB-treated and P-doped/AB-treated hematite photoanodes. The spectrum of the P-doped/AB-treated sample indicates the P-doping. The small pre-peak A clearly reveals the existence of $FePO_4$ in the sample.

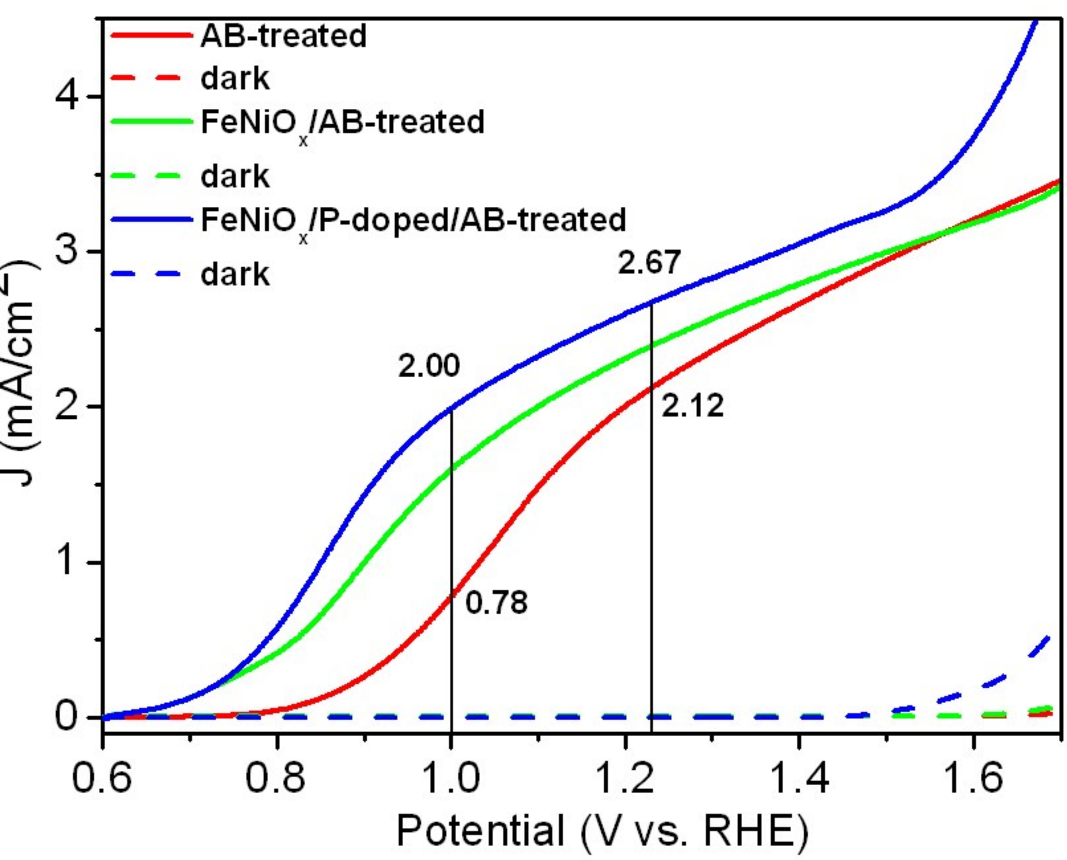

Figure S7: *J-V* scans of the AB-treated, $FeNiO_x$/AB-treated and $FeNiO_x$/ P-doped/AB-treated hematite photoanodes.

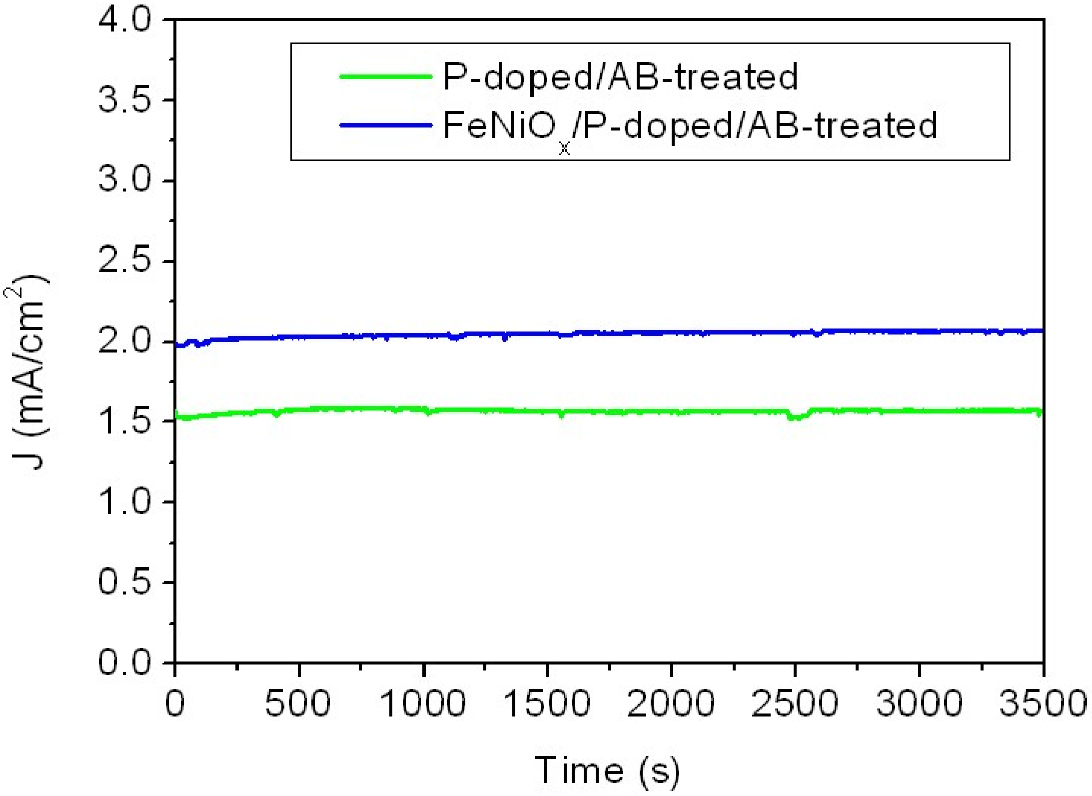

Figure S8: Photochemical stability curves of the P-doped/AB-treated and FeNiO$_x$/ P-doped/AB-treated hematite photoanodes collected at 1.0 V vs. RHE.

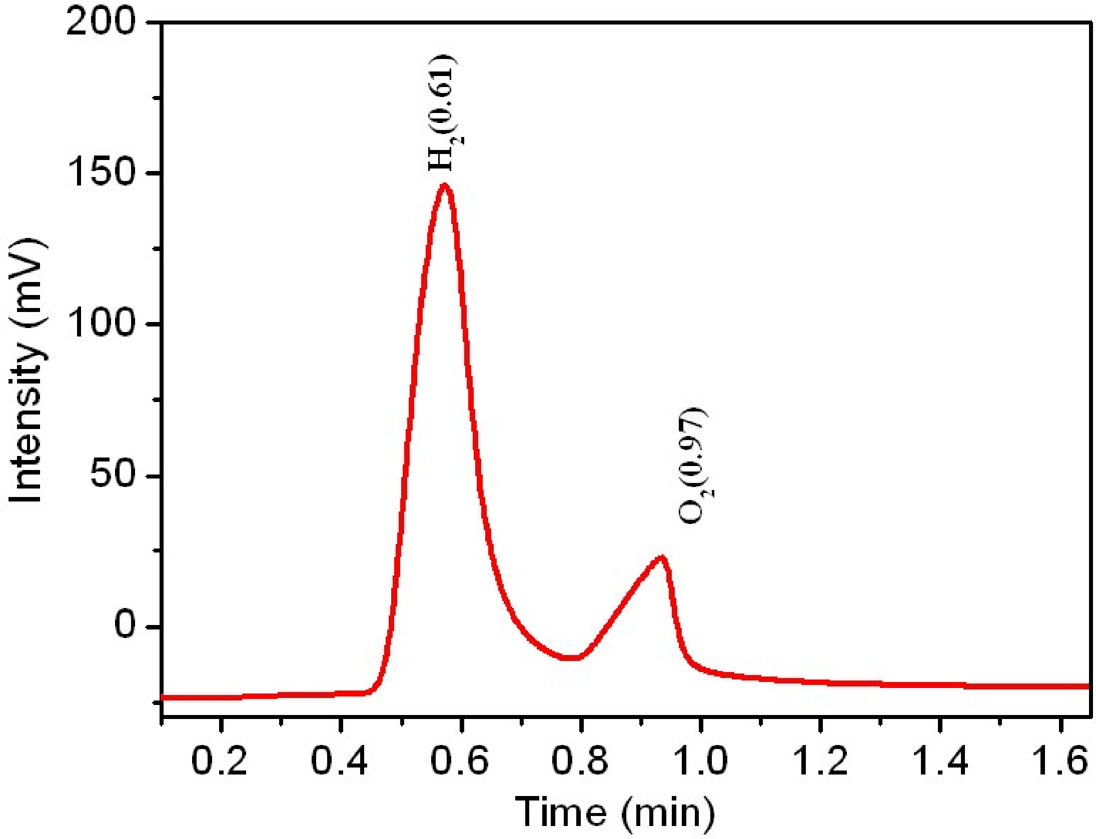

Figure S9: Final product detection using a gas chromatograph (GC7890T system, using N_2 as carrier gas and the TCD temperature was set to be 130 °C). H_2 and O_2 can be clearly detected confirming the product.

Sample description	Preparation method	Further modifications	Photocurrent (mA/cm^2) at 1.0 V *vs.* RHE	Journal and year
3D-Fe_2O_3 nanocore	Ultrasonic spray pyrolysis	Ti-doping/Au layer/Co-Pi catalyst	2.6	Energy Environ. Sci. 2014, Ref. 21
Fe_2O_3	Hydrothermal method	Pt-doping/Co-Pi catalyst	2.3	Sci. Rep. 2013, Ref. 33
Hydrogenated- Fe_2O_3	Hydrothermal method	P-doping/$FeNiO_x$ catalyst	2.0	**This work**
3D-Fe_2O_3 nanospiked array	Ultrasonic spray pyrolysis	Ti-doping/Co-Pi catalyst	2.0	Nano Lett. 2014, Ref. 20
1D Fe_2O_3 grown on 3D Sb-doped SnO_2	Hydrothermal method	TiO_2 layer/Co-Pi catalyst	2.0	Adv. Sci. 2015, Ref. 34
Fe_2O_3	Deposition-annealing process	Ti-doping	1.75	Nano Lett. 2011, Ref. 17
Fe_2O_3	Hydrothermal method	P-doping/Co-Pi catalyst	1.6	Energy Environ. Sci. 2015, Ref. 15
Fe_2O_3	APCVD	Al_2O_3 layer/$FeNiO_x$ catalyst	1.5	J. Am. Chem. Soc. 2015, Ref. 14
Fe_2O_3	APCVD	IrO_2 catalyst	1.2	Angew. Chem., Int. Ed. 2010, Ref. 5
Re-growth Fe_2O_3	Hydrothermal method	$FeNiO_x$ catalyst	1.05	Nat. Commun. 2015, Ref. 3
Fe_2O_3	APCVD	Co-Pi catalyst	1.0	Energy Environ. Sci. 2011, Ref. 4
Fe_2O_3	Electrochemical deposition	Sn-doping/Co^{2+} catalyst	1.0	J. Mater. Chem. A 2015, Ref. 35
Fe_2O_3	Hydrothermal method	Sn and Zr codoping/ NiOOH catalyst	1.0	J. Mater. Chem. A 2015, Ref. 36
Fe_2O_3	Hydrothermal method	Carbon coating	0.9	Energy Environ. Sci. 2013, Ref. 22
Fe_2O_3	Hydrothermal method	------	0.8	Nano Lett. 2011, Ref. 11
Fe_2O_3	Hydrothermal method and hybrid microwave annealing	------	0.8	ACS Appl. Mater. Interfaces 2015, Ref. 26
Fe_2O_3	Hydrothermal method	Ti-doping/$Ni(OH)_2$ and IrO_2 cocatalyst	0.8	J. Phys. Chem. C 2015, Ref. 37
Fe_2O_3 grown on patterned FTO	Hydrothermal method	------	0.7	J. Mater. Chem. A 2015, Ref. 38
Fe_2O_3	Hydrothermal method	$Fe_xSn_{1-x}O_4$ layer	0.65	Chem. Sci. 2013, Ref. 39
Fe_2O_3 grown on Si nanowire array	Atomic layer deposition	------	0.63	J. Am. Chem. Soc. 2012, Ref. 40
Fe_2O_3 Nanoflake array (1D)	Thermal oxidation of iron foil	Au decoration	0.5	ChemSusChem 2015, Ref. 41
Fe_2O_3 with oxygen vacancies	Hydrothermal method	------	0.2	Angew. Chem., Int. Ed. 2012, Ref. 18

Table S1: Comparison of the photocurrent densities of hematite photoanodes at 1.0 V *vs.* RHE.